Technology in Cancer Research and Treatment
ISSN 1533-0346
Volume 13, Number 6, December 2014

Commissioning of an Integrated Platform for Time-Resolved Treatment Delivery in Scanned Ion Beam Therapy by Means of Optical Motion Monitoring

www.tcrt.org
DOI: 10.7785/tcrtexpress.2013.600275

The integrated use of optical technologies for patient monitoring is addressed in the framework of time-resolved treatment delivery for scanned ion beam therapy. A software application has been designed to provide the therapy control system (TCS) with a continuous geometrical feedback by processing the external surrogates tridimensional data, detected in real-time via optical tracking. Conventional procedures for phase-based respiratory phase detection were implemented, as well as the interface to patient specific correlation models, in order to estimate internal tumor motion from surface markers. In this paper, particular attention is dedicated to the quantification of time delays resulting from system integration and its compensation by means of polynomial interpolation in the time domain. Dedicated tests to assess the separate delay contributions due to optical signal processing, digital data transfer to the TCS and passive beam energy modulation actuation have been performed. We report the system technological commissioning activities reporting dose distribution errors in a phantom study, where the treatment of a lung lesion was simulated, with both lateral and range beam position compensation. The zero-delay systems integration with a specific active scanning delivery machine was achieved by tuning the amount of time prediction applied to lateral (14.61 ± 0.98 ms) and depth (34.1 ± 6.29 ms) beam position correction signals, featuring sub-millimeter accuracy in forward estimation. Direct optical target observation and motion phase (MPh) based tumor motion discretization strategies were tested, resulting in $-0.3(2.3)$% and $-1.2(9.3)$% median (IQR) percentual relative dose difference with respect to static irradiation, respectively. Results confirm the technical feasibility of the implemented strategy towards 4D treatment delivery, with negligible percentual dose deviations with respect to static irradiation.

Key words: Tumor tracking; Optical tracking system; Beam tracking; Real time; Particle therapy.

G. Fattori, M.Sc.[1]*
N. Saito, Ph.D.[2]
M. Seregni, M.Sc.[1]
R. Kaderka, Ph.D.[2]
A. Pella, Ph.D.[3]
A. Constantinescu, M.Sc.[2]
M. Riboldi, Ph.D.[1,3]
P. Steidl, Ph.D.[2]
P. Cerveri, Ph.D.[1,3]
C. Bert, Ph.D.[2,4]
M. Durante, Ph.D.[2,5]
G. Baroni, Ph.D.[1,3]

[1]Dipartimento di Elettronica Informazione e Bioingegneria, Politecnico di Milano, P.zza Leonardo da Vinci 32, 20133 Milano, Italy
[2]GSI Helmholtzzentrum für Schwerionenforschung GmbH, Abt. Biophysik, Planckstraβe 1, 64291 Darmstadt, Germany
[3]CNAO Centro Nazionale di Adroterapia Oncologica, Strada privata Campeggi 53, 27100 Pavia, Italy
[4]University Clinic Erlangen, Radiation Oncology, Universitätsstraβe 27, 91054 Erlangen, Germany
[5]TU Darmstadt, Hochschulstraβe 6, 64289 Darmstadt, Germany

Introduction

Intra-fractionally moving targets represent approximately 17% of diagnosed cancer malignancies in USA (1). Among them, non-metastatic solid tumors such as lung and pancreas lesions represent a potentially eligible population for ion beam therapy, for which current limitations in motion compensated delivery hinder actual clinical application. The ability to overcome such limitations may contribute to improve the cost-benefit ratio of particle therapy facilities in upcoming

Abbreviations: BTU: Beam Tracking Unit; CT: Computed Tomography; IQR: Inter Quartile Range; LUT: Look-up Table; MPh: Motion Phase; MPhT: Motion Phase Table; OTS: Optical Tracking System; RCS: Room Coordinates System; TCS: Therapy Control System; TVC: Tele-video Camera.

*Corresponding author:
G. Fattori, M.Sc.
E-mail: giovanni.fattori@polimi.it

years, with potential benefits in terms of local tumor control for patients with poor prognosis (2-5).

As a matter of fact, despite the noteworthy research efforts to handle motion-induced uncertainties in treatment plan optimization (6) and delivery (7-9), the effective clinical treatment of moving lesions with active beam scanning is still a challenge (10-11). The main reason is the need to deal with deviations in the motion patterns at the treatment time with respect to the treatment planning dataset, as resulting from the patient specific inter- and intra-fraction variability. In this perspective, accurate in-room motion monitoring, featuring quasi real-time target motion assessment is mandatory in order to check whether the treatment planning 4DCT imaging conditions are maintained to deliver a time-resolved treatment plan (12-15). Different motion mitigation techniques have been proposed over the years, depending on the available dose delivery and on the expected patterns of target motion. In-room motion monitoring systems are intended to play a key role during treatment, providing the therapy control system (TCS) with the gating signal (8, 16-18), as well as the real-time tumor position for beam tracking (9, 19-21).

Approaches to direct tumor motion observation relying on on-line imaging have been recently described (22-25). However, the additional dose delivered to the patient limits usage of continuous in-room imaging for long-term patient surveillance. On the other hand, non-ionizing technologies, which allow for high-frequency motion monitoring, typically provide breathing surrogate signals instead of direct tumor position. This is the case of devices such as video-based system (Varian RPM), elastometers (Anzai Belt), infrared localizers or laser distantiometers (26-28). Recently, the combined use of devices for monitoring surface surrogates and patient-specific modeling for external-internal correlation estimation, as trained by periodic image acquisition during treatment, has been proposed as the optimal trade off in terms of accuracy and frame rate (Figure 1) (29, 30). This technique has been applied clinically since the early 2000s in conventional X-ray radiotherapy, where the uncertainties in dose deposition due to motion are less restrictive (31). From a technical standpoint, the heterogeneous nature of in-room imaging systems in particle therapy facilities, as well as the strict tolerance margins in dose painting, make the transfer of the technological know-how from image guided photon therapy to scanned ion beams hard to achieve. The real-time integration of information coming from different motion monitoring and imaging systems in the treatment room represents a necessary requirement for the implementation of any motion-correlated or motion-compensated irradiation strategy. Such integration embodies the technological and methodological framework for the development and experimental validation of patient-specific correlation models to be used for motion compensated treatments.

In this work we present the implementation, commissioning and experimental testing of a dedicated technical platform to assess and communicate real-time motion signals to a TCS for tumor tracking in active scanning ion beam therapy. The design is specifically suitable for beam tracking, where compensation methods for beam steering and energy adaptation feature a different reaction time (32). The system is validated integrating a real-time infrared (IR) optical tracking system (OTS) with the GSI (Helmholtzzentrum für Schwerionenforschung) TCS for scanned ion beam therapy of moving targets, aiming at effective motion mitigation in free breathing. We describe a phantom study designed to assess the technical performance in a nearly clinical scenario, providing the TCS alternatively with real-time information on the motion phase (MPh) or the 3D position of the moving target. While the benchmark of correlation models has been already presented elsewhere (33), here we focus on the technical performance assessment and system commissioning that were addressed in experimental trials for the quantification of specific contributions to the dose delivery reaction delay.

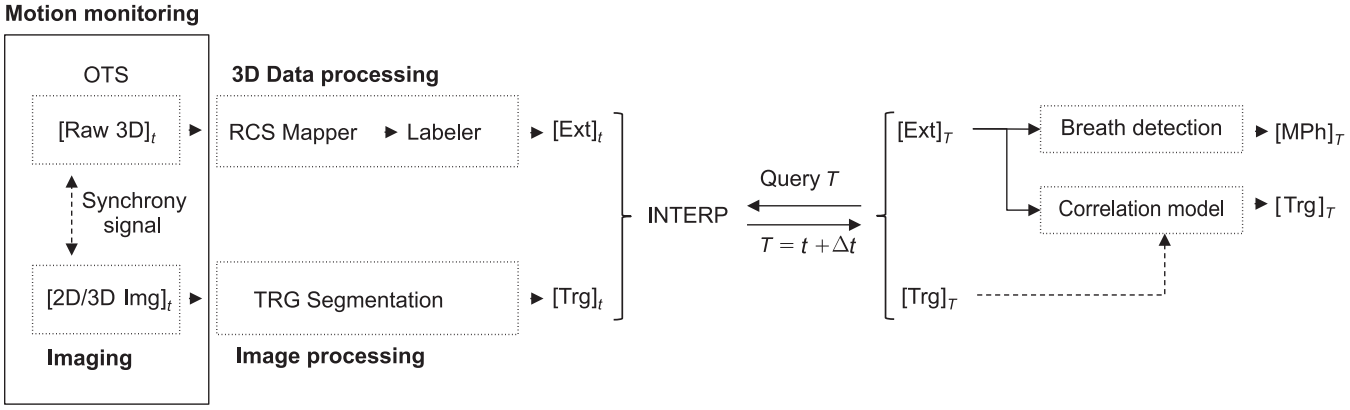

Figure 1: Software application schematic diagram.

Materials & Methods

Time-resolved treatment planning includes the overall set of pre-calculated dose delivery settings to be applied at each irradiation spot, as a function of actual observed patient geometry. This, under the assumption of target motion repeatability, is typically handled by sampling tumor motion in a defined reduced number of bins/phases, to be detected during treatment by in-room monitoring systems. When focusing on beam tracking, it is mandatory to account for the different reaction time required for (i) beam deflection according to motion and (ii) energy adaptation as a function of the variable tissue density along the beam path.

In the following we detail systems setup activities towards a MPh based treatment delivery, as well as the usage of continuous target position for lateral beam deflection in the perspective of time resolved delivery relying on internal/external correlation models. In the proposed phantom study, optical technologies have been exploited for both external and target surrogates tracking. In such a way we tested the capability of the system independently of X-ray in-room image acquisition and real-time processing, which are required for target delineation at treatment time.

The Optical Tracking System

The general-purpose point-based infrared OTS SMART-DX100 (BTS-Bioengineering, Garbagnate Milanese, Italy) was used as motion detection platform. This is a commercial off-the-shelf solution for infrared motion capture, which was configured with three Tele-Video Camera (TVC) in our study setup. The system is designed for human movement analysis and provides tools for 3D reconstruction of IR-reflective coated spherical markers at nominal 100 Hz frame rate. The preliminary calibration procedure involves user interaction and takes about 15 min, resulting in sub-millimetric reconstruction accuracy in a cubic meter working volume (34). The in-room calibration procedure relying on a qualified calibration phantom was developed to map three-dimensional optical data in a room coordinates system (RCS). We used the BrainLab (BrainLAB AG, Feldkirchen, Germany) phantom, which is specifically designed to be manually aligned to the room iso-centric lasers and is fitted with a set of OTS compatible markers in known position with respect to the phantom geometrical center. The mapping matrix is calculated by rigidly registering the nominal coordinates and the in-room acquired phantom markers by means of singular values decomposition least square optimization (35). The point correspondence is achieved with a pre-optimization step designed for data sorting, by means of principal components analysis projection of both dataset, providing nearest neighborhood marker labeling prior to the optimization function.

A dedicated software application handles the optical real-time data flow, ensuring a continuous time resolved geometrical feedback to the TCS during the whole treatment delivery. The network UDP datagram protocol has been adopted for OTS/TCS data transfer. The information for beam in-plane correction and energy modulation is then made available for the beam tracking unit (BTU) by shared memory, via a dedicated interface routine, since multiple motion monitoring devices and protocols are supported by the core-program of the TCS.

Data Processing

The implemented system is designed to provide a geometrical feedback to the TCS at user-defined frequency during treatment delivery. Markers in free motion are tracked by labeling the raw OTS data with respect to the patient-specific model. The pre-requisite is that a configuration of radio-opaque, IR-reflective markers is fitted to the patient (or to the phantom in our case) during the treatment planning CT scan acquisition. The position of surface fiducials detected in the CT and expressed in the imaging reference system, represents the reference treatment geometry (34). In order to ensure the correct tracking of visible markers over time, the point-based patient model is continuously updated during the acquisition. The nominal model, which is initially loaded for positioning purposes, is actualized at each frame by proximity-based marker matching. The Euclidean 3D distance is considered as metric and the nearest neighbor is found by means of a brute force searching algorithm, which cycles over all markers in the scene and searches for the nearest fiducials on the model under a pre-defined 3D distance threshold.

In order to ensure accurate real-time feedback, the data retrieval and frame processing procedures are executed in parallel with appropriate priority. In particular, the latest 5 available frames define the time-span for interpolation, with fitting coefficients update at each incoming frame. Frames interpolation is performed on single marker coordinates, as stored in the buffered frames, by least square fitting with linear polynomial curves. A real-time priority thread, running at user defined frequency, extrapolates a virtual frame from the real frames interpolation, which is then considered for further processing and feedback to TCS. Moreover, time prediction can be performed separately on each marker coordinates, to form the $t + \Delta t$ virtual frame, where Δt is the requested prediction ahead to be considered. This implementation allows the user to define a specific time prediction for MPh signal and 3D correction vector, in order to compensate for additional delays in data communication and specific dose delivery systems reaction times for lateral and range beam modulation.

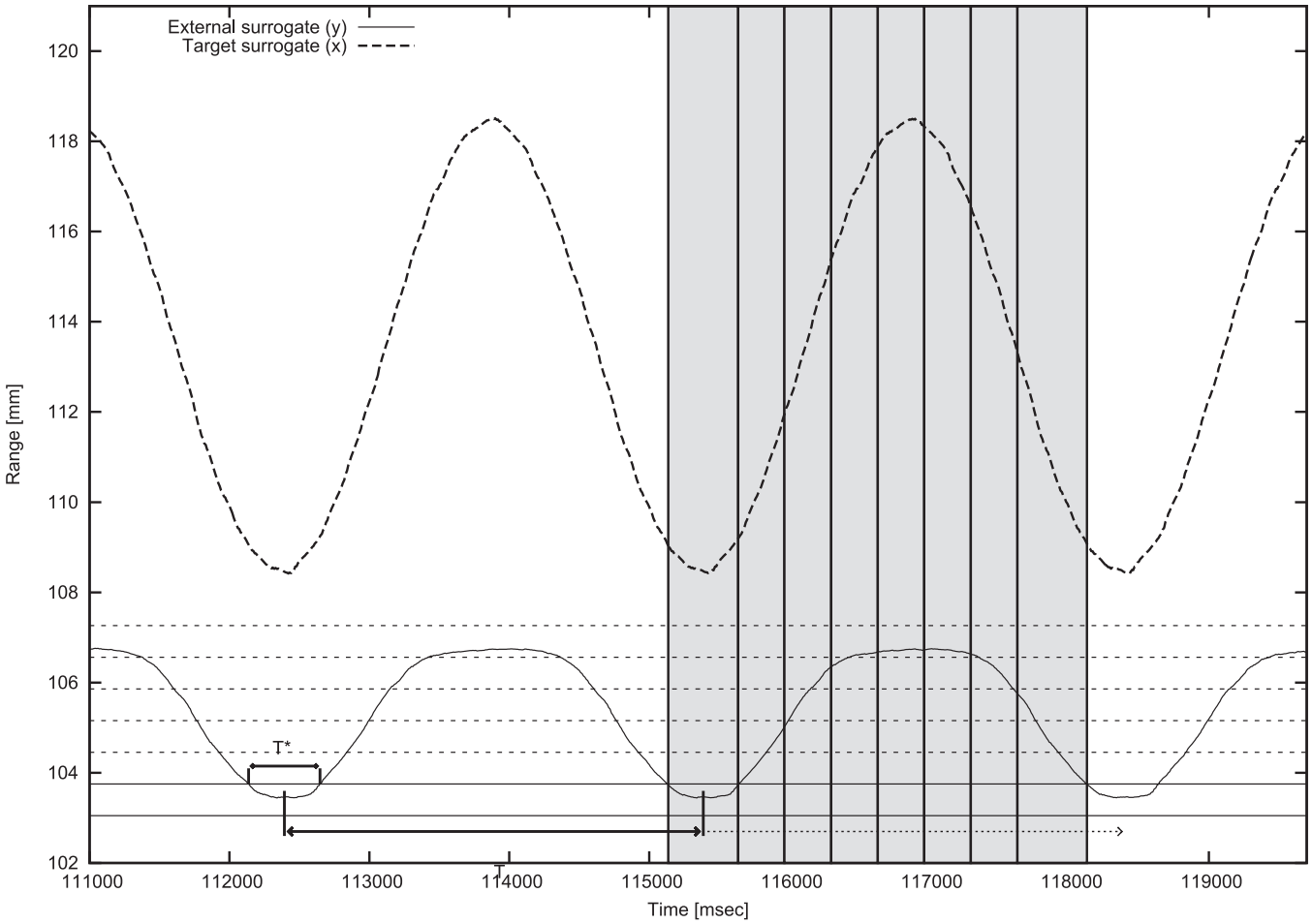

Figure 2: MPh detection algorithm. Target motion (dashed curve) and breathing surrogate signal (solid curve) with amplitude phase binning (dotted lines) and end-exhale instants detection as the midpoints of the time intervals in which the breathing surrogate signal is located in the lowest amplitude-based MPh bin. Resulting phase-based bins are highlighted in grey.

Both amplitude- and phase-based MPh detection algorithms have been implemented to provide motion feedback for beam tracking and gating (Figure 2) treatment modalities. The amplitude-based MPh binning table (MPhT) is created from the configuration of radio-opaque markers, which are segmented in the 4DCT dataset. In order to provide robust MPh classification even in presence of noise and motion irregularities we have considered the AP projection of the surface marker with the largest range of motion. The algorithm starts the classification only after having recorded the MPh corresponding to the most posterior position (*i.e.* end of exhale). Then, new frames are classified comparing the observed coordinates with the actual or subsequent MPhT bin. The maximum number of forward MPhs to be considered in the search can be set by the user. The phase-based MPh binning LUT is constructed as percentage values with respect to the nominal breathing period, thus defining the bounds for each MPh. The synchronization with the real-time measured respiratory signal is achieved through the amplitude-based identification of end-exhale instants (Figure 2).

Beside the MPh detection, current implementation includes two correlation models designed for tumor tracking in scanned ion therapy. A computationally lightweight approach such as a space state model allows for real-time training and frame processing in the main routine (29). Otherwise, models that include demanding training functions are required to run on a separate hardware to avoid affecting the data acquisition frame rate. This is the case of the neural network model, which features a mirrored implementation on the OTS workstation and a dedicated training machine. Frames comprehensive of external surrogates and target position are sparsely made available to the selected model and considered for performance benchmark. If the error is above a pre-defined threshold, a number of frames are collected and provided to the training machine by network file sharing, as described by Seregni *et al.* (33). While the model is being trained, the

TCS is alternatively provided with a beam pause signal or the output of the currently running model.

Experimental Setup and Measurement of System Delays

The above described OTS and related application was interfaced to the environment featuring 4D compliant TCS (20, 36) and treatment planning system (TPS) available at GSI (6, 37). The present dose delivery system is extensively described in previous studies in terms of accuracy, speed and dosimetric aspects (7, 32, 36). Dedicated tests to assess the separate delay contributions due to OTS processing, UDP data transfer and wedge range shifter acceleration were performed (Figure 3). The requirements for optical frames processing and digital communication time were quantified by benchmarking the use of the OTS motion monitoring system with the OD100-35P840 real-time (1 KHz sampling rate) laser distantiometer (SICK AG, Waldkirch, Germany). A sliding table in sinusoidal motion (Figure 3) with a 3 sec period was tracked relying on both systems for comparison. According to Saito *et al. (*38) the voltage signal encoding for the laser measured distance is digitalized and provided to the TCS by the analog to digital converter (Model VMOD-12E16, Janz Computer AG, Germany). The dephasing over signals resulting from the coupled OTS-Laser observation of sliding table motion was considered as a measure of the time lag introduced by the OTS frames processing and the digital communication to the TCS. For data analysis purposes, the experimental asynchronous optical and laser data series were resampled at a given constant sampling rate (1 KHz) with cubic spline interpolation and filtered for signal smoothing. We considered a 20th order normalized low-pass FIR filter at 2E-6 cut-off frequency, followed by a zero-phase forward digital IIR filter. The phase difference estimation was based on FFT calculation of the two signals. Linear interpolation was applied in the frequency domain in order to identify the phase in correspondence of the nominal frequency for each signal and the difference was considered as dephasing measurement. The relationship between the imposed time prediction and the effective measured delay was investigated in five experimental trials with different tracking forward time prediction equal to 0, 5, 10, 15, 20 msec.

Once available at the TCS level, the lateral components of the correction vector are actuated in millisecond time scale by lateral beam deflection (32); conversely, the ion beam range modulation required further investigation as a function of the specific treatment plan considered for the subsequent dosimetric study. The delay introduced by the movement of the wedge filter was quantified by a similar setup with the sliding table described above. For this particular experiment, an IR-reflective marker was mounted on the wedge and optically tracked. The periodic table motion was considered as input for the detection of 10 MPh, evenly spaced in amplitude, so that measurements up to 9 mm water equivalent path length were performed in steps of 1 mm. The mean time elapsed from the detected MPh change and the optically observed wedge actuation was considered as the time required for beam range modulation. This value was calculated by identifying the wedge actuation through sudden variations in the wedge surrogate position over time. The total time subtracted by the already estimated OTS processing and communication time requirements was considered as the mean wedge reaction time for 1 and 9 mm WE ion beam range compensation.

Signal Time Prediction Accuracy

The additional uncertainty affecting the three-dimensional optical measurement, due to interpolation and time prediction was quantified in a phantom study. The setup was representative of a nearly clinical scenario and relied on the GSI manufactured anthropomorphic breathing phantom, featuring synchronized motion of an internal target, which mimics a lung lesion and a torso model (Figure 4) (39). We considered the time-labeled 3D data belonging to the target surrogate moved along an ellipsoidal trajectory with 10 and 5 mm peak-to-peak amplitude in the (x, y) plane and 10 mm range along the beam eye view direction.

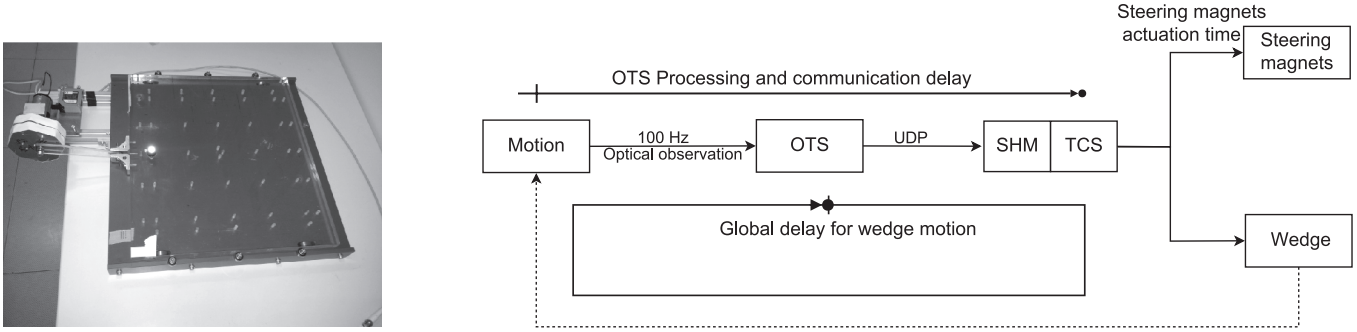

Figure 3: Performance study setup: sliding table (left panel) and schematic of delay test actors (right panel).

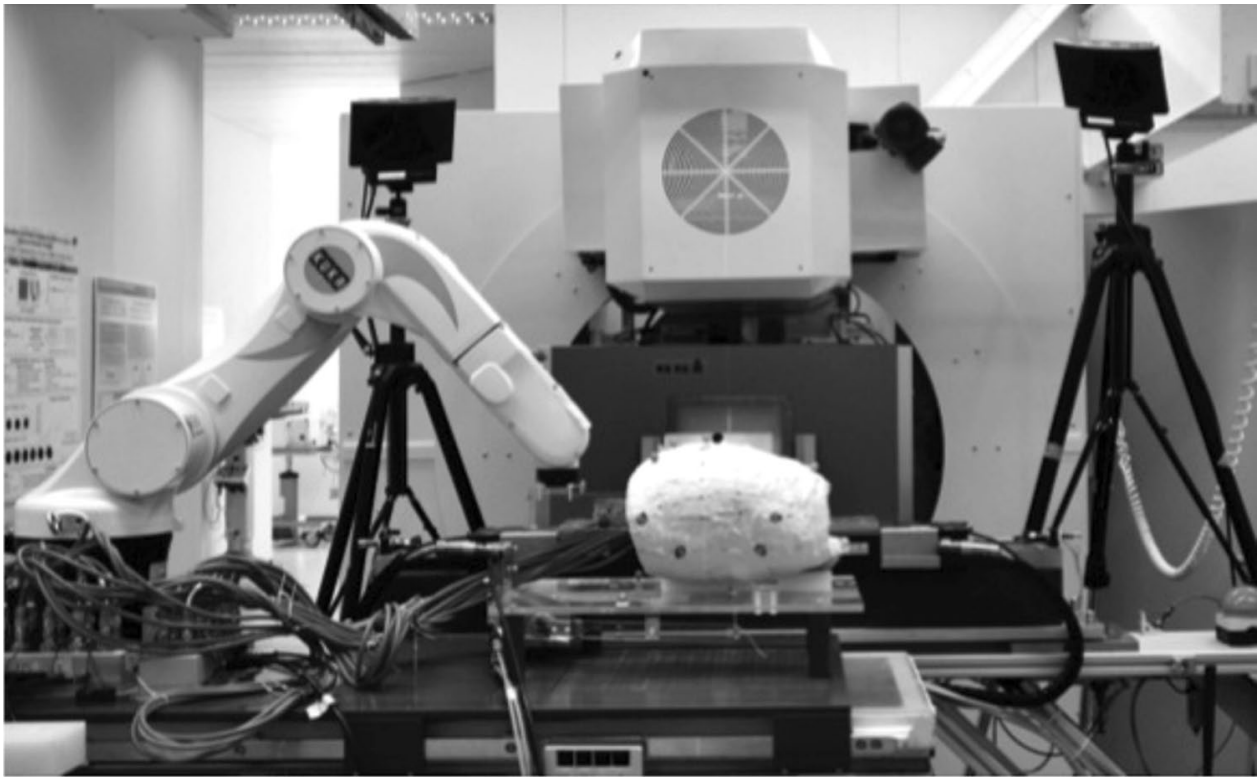

Figure 4: Experimental study setup.

The OTS observed target position signal, shifted in time by optimized prediction according to the outcomes of the above described performance study (Cfr. Experimental setup and measurement of system delays) was considered as the reference signal. Real time fiducial reconstruction uncertainties were calculated as the difference between the reference time-compensated motion trajectory and OTS data, with and without polynomial time prediction. The raw OTS dataset sampling rate was considered as time grid for signal interpolation, thus providing a time consistent set of overlaid signals. Root mean square error and inter-quartile range of signals differences distribution were quantified as a measure of uncertainties affecting beam tracking signals flowing from the OTS to the TCS.

Phantom Irradiation

The capabilities of the implemented motion monitoring framework were assessed in a phantom study, designed to compare the delivery of time-resolved treatment plan and the static irradiation by comparing the readout of 16 ionization chambers embedded in the lung lesion of the phantom. We fitted the thorax phantom described above with a configuration of 5 fiducials (2 apical, 3 proximal), 3 additional landmarks were placed on the supporting framework. The planning 4 DCT was acquired as a series of static CT pausing the phantom motion at known time intervals. The dataset comprehensive of 8 MPh feature 0.7 mm in-plane pixel spacing and 3 mm slice thickness. Radiopaque surface fiducials were automatically localized in the CT image (34) and mapped in the RCS following a frameless stereotactic approach (40). The 4D treatment plan was optimized (37, 41) by considering 1 Gy homogeneous dose deposition in a 35 mm side cubic PTV, enlarged through a total isotropic contour extension of 0.7 mm. Considering the 6 mm beam FWHM, this resulted in an effective overlap between the phantom pinpoint holder (5 cm side) and the PTV volume (4.2 cm side).

The experimentally calculated amount of forward prediction for compensating OTS processing and data communication to TCS was applied to all tracked surrogates in the scene. The MPh signal provided to the range modulation filter underwent an additional prediction equal to the time required for the MPh change duration, as measured in the performance study setup (Cfr. Experimental setup and measurement of system delays).

The integrated OTS-TCS system was tested under two modalities, which differed in the content of the feedback provided to the TCS:

- MPh based strategy: a fully LUT based approach providing the TCS with two MPhs signals, with different time prediction, for lateral and depth corrections. At treatment

time, the TCS selected on the fly the values for lateral and depth beam position correction on a spot-by-spot basis from the beam correction table pre-calculated at treatment lanning (37).

- Direct lateral target position and depth MPh encoding: the experimental phantom setup allowed the OTS to track continuously a surrogate marker fixed on the target. The directly observed target coordinates expressed in the RCS were sent to the TCS for continuous lateral compensation; the MPh signal encoding was used for beam depth compensation as in the previous experimental condition.

The ionisation chamber based dose measurements resulting from a preliminary static irradiation experiment without phantom motion were considered as reference for the evaluation of the dosimetric effect of 4D treatment delivery.

Results

Experimental Setup and Measurement of System Delays

The experimental data points of measured OTS-Laser signals dephasing at different time prediction were linearly fitted featuring $R^2 = 0.98$. The trend line was considered for the extrapolation of the prediction time, allowing for a theoretical zero-delay systems interaction (Figure 5). The analysis reported 14.61 ms delay, which was selected as the optimal value to be set in the tracking application for prediction.

The wedge performance study lasted 79.4 sec and allowed for data log acquisition comprehensive of 27 and 243 measurements for 9 and 1 mm WE compensation, respectively. The mean wedge filter actuation time, subtracted by the bias due to OTS processing and communication time is equal to 27.43 $\pm$ 7.51 ms for each MPh step (1 mm WE) and 34.1 $\pm$ 6.29 ms for the larger compensation (9 mm WE). No data loss was observed in the UDP communication and 100% data transfer was reported by the TCS reader.

Signal Time Prediction Accuracy

About 10 min acquisition generated an error distribution with a [0.06, 0.18 mm] 25th-75th inter quartile range (IQR), (Figure 6 right panel). The corresponding RMS values were 0.05 and 0.1 mm for time predicted and non-predicted signals, respectively.

In the lower left panel of Figure 6 we report the error distribution as a function of time over two breathing cycles, providing a visual representation of the relationship between the error distribution and the observed motion trace.

Phantom Irradiation

Percentual dose difference measurements have been tested for normality by means of single sample Kolmogorov-Smirnov test. The null hypothesis of data normality has been rejected within 1% confidence on both interplay (ks-statistic: 0.5432; *p*-value: 5.9581e-05) and MPhT (ks-statistic: 0.4819; *p*-value: 6.0971e-04) approaches. Conversely, direct target observation measurements exhibited a standard normal distribution (ks-statistic: 0.2765, *p*-value: 0.1423). Therefore,

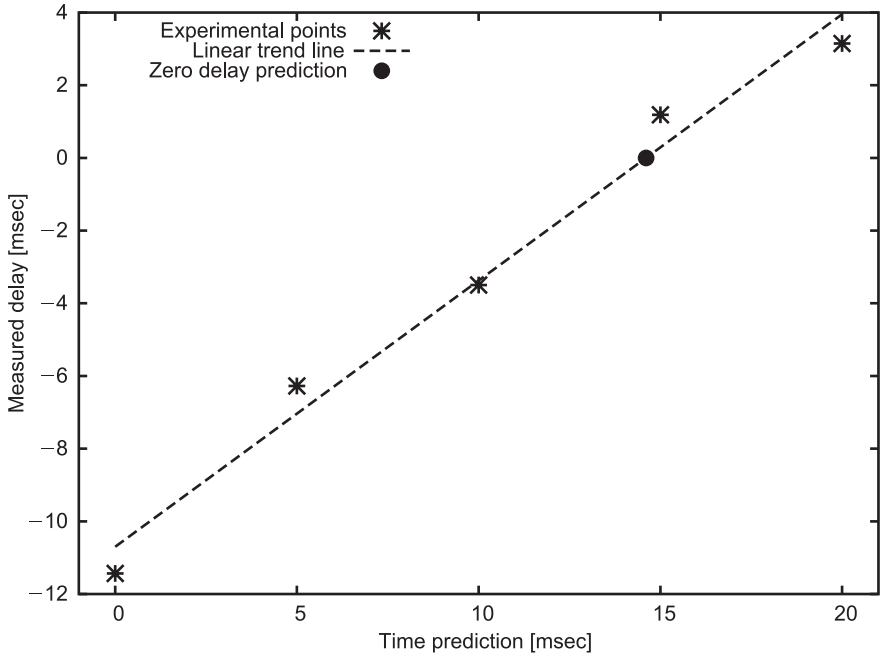

Figure 5: Measured systems delay as function of imposed time prediction.

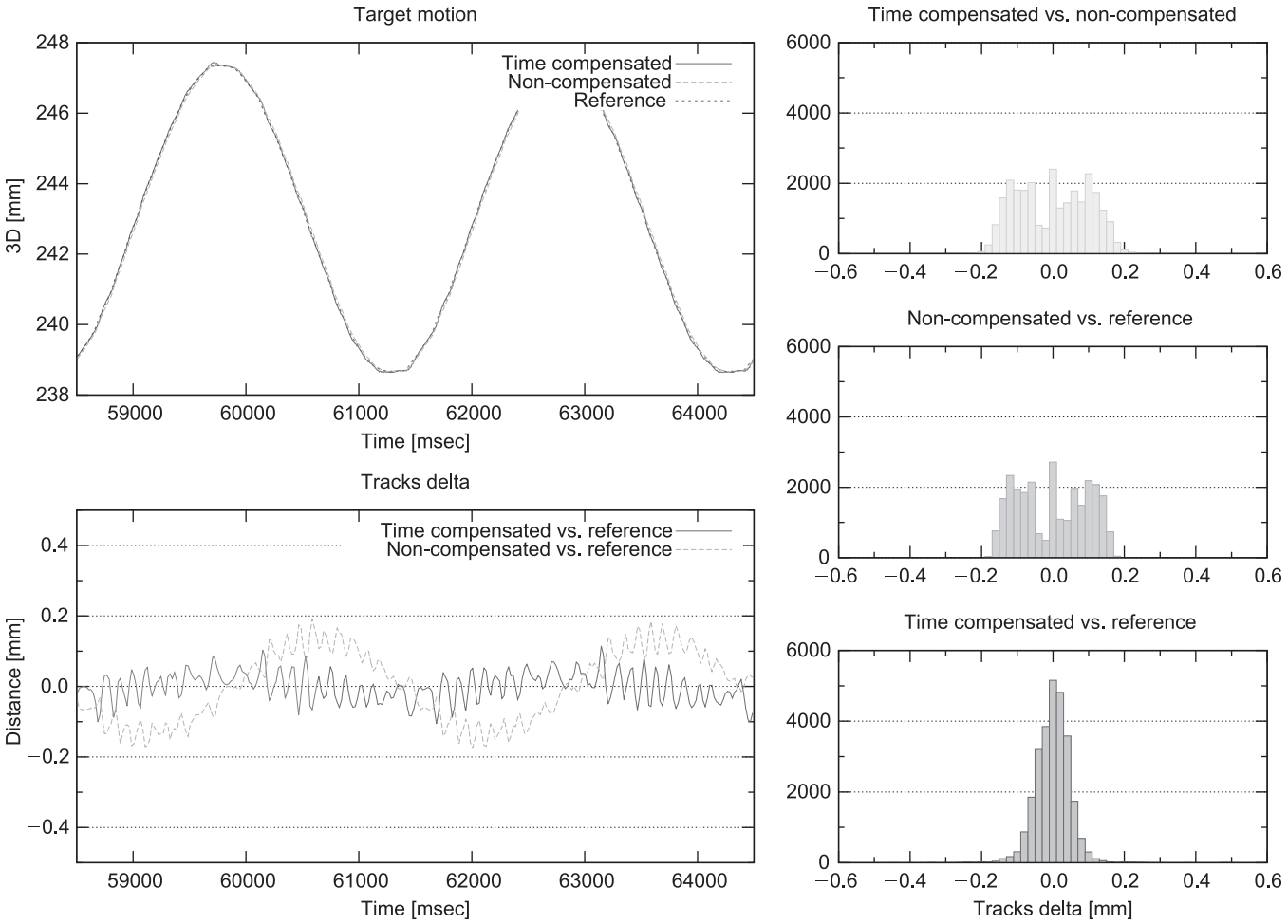

Figure 6: Interpolation and time prediction accuracy. Left panel: reference, time-compensated and non-compensated signals overlay (top), time-compensated and non-compensated delta wrt reference (bottom) for two breathing cycles; Right panel: Error distribution for compensated wrt non-compensated (top), non-compensated (middle) and compensated (bottom) wrt reference.

for comparison purposes, a description of delivered dose is provided as median percentual dose deviation with respect to the static irradiation. The difference between the 75th and 25th percentiles is reported as in index of the dose degradation in target coverage (Table I). The overall picture of dosimetric measurements is depicted in Figure 7, that reports the box plot of the dose differences on all ionization chambers for each experimental condition.

Table I

Percentual dose difference with respect to the static irradiation, median and IQR values.

ID	Lateral	Depth	Median (IQR)
Interplay	x	x	2.0 (25.9) %
Direct	Direct	MPh	−0.3 (2.3) %
MPh	MPh	MPh	−1.2 (9.3) %

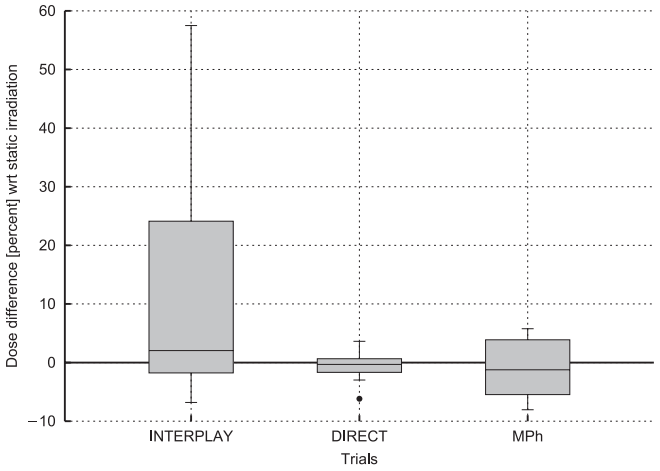

Figure 7: Dose difference with respect to the static irradiation on all ionization chambers.

Discussion

A technical framework for optically driven 4D treatment delivery was tested in the framework of scanned ion beam therapy. The results of the experimental commissioning of dedicated procedural and technological solutions for IR motion monitoring and real-time communication to the beam tracking system were reported. The overall set of technologies and methods was optimized to achieve real-time breathing motion compensation and fast communication to the delivery machine. A stand-alone application exploiting the real-time 3D data flow coming from the OTS was implemented, providing procedures for system setup in the treatment bunker and real-time elaboration of motion tracking information. The integrated system latencies and communication delays were quantified both for lateral and depth motion compensation. Two different motion compensation strategies, *i.e.* MPh based correction and continuous target tracking, were experimentally assessed, providing dosimetric results.

Accurate patient alignment is the preliminary requirement towards the accurate delivery of the treatment plan and in-room treatment geometry consistency. Errors in patient setup can severely affect the overall quality of the treatment, particularly in case of time-resolved treatments, which requires an agreement between treatment plan and irradiation geometry over the complete breathing cycle. In our study, the landmarks on the phantom thorax surface have been considered for in-room registration in a frameless stereotactic approach. The consistency of breathing motion between treatment planning and dose delivery was ensured by the phantom motion repeatability, whereas in clinical practice the synchronization of imaging devices with the patient breathing cycle is crucial. The detailed platform, feeding the imaging system with information about observed motion, can potentially trigger the acquisition to correlate image data with patient breathing motion. Such a correlated dataset can be used to build a proper correlation model between external surface motion and the internal target trajectory, or to check the performance of an existing model based on prior knowledge (such as the treatment planning 4D CT or a previous imaging session). The described approach is similar to what is currently implemented in commercial systems applied in conventional photon radiotherapy, providing a quantitative method to check inter- and intra-fraction variations in the breathing pattern, aiming at the maximal accuracy in dose delivery.

Concerning the motion capture, it is worth considering that time interpolation at a fixed sampling rate was required, due to the intrinsic variability of the optical frame processing over long time acquisitions. Our implementation allowed us to count on a stable motion data communication at 100 Hz, which was obtained from a 50 Hz OTS acquisition. The interpolated data stream could be handled adequately by the UDP communication and resulted in a 100% OTS/TCS data transfer. This yields appropriate time resolution in the geometrical feedback to TCS, compared to a raster scanning speed of 10 ms between adjacent irradiation points.

OTS processing and communication delays were faced by time prediction relying on polynomial data fitting. The quality of the implemented prediction strategy depends on (i) the observed motion and (ii) the size of the required forward estimation in time. The component of the normal breathing signal spectrum to be considered is the respiration fundamental frequency, which is about 0.3 Hz in normal breathers. The OTS high sampling rate allows for signal prediction in a neighborhood of the interpolator as reported in the corresponding benchmark study (Cfr. Signal time prediction accuracy). The comparison of error distributions of time compensated and uncompensated signals with respect to the reference data showed that the time-compensated signal exhibited minimal discrepancies in rising and falling edges, with a slight increased error in peaks detection due to the 5 samples history used for time prediction. As a matter of fact, the need to collect adequate data history for time interpolation is a potential source of dephasing in case of high frequency signal variations within the buffered data. Such an effect is expected to be minimal for the prediction of normal breathing induced motion, whereas sudden changes (such as patient coughing) should be treated carefully in motion compensation strategies. The implemented framework allows setting geometrical constraints on the observed motion and reacting immediately to unexpected situations by pausing the beam through RF knockout.

The different technological implementation for lateral and depth beam adjustment, featuring different reaction times, required specific time prediction on the signals provided to the TCS. Dedicated tests were performed aiming at the tuning of predictors parameters for the optimal compensation of OTS processing and digital communication time. Additional time prediction was applied for depth compensation, in order to account for the time required for passive filter actuation for beam energy modulation. The proposed approach for signal comparison relying on dephasing analysis provided accurate OTS delay quantification. This allowed us to characterize the relationship between the requested and actually obtained prediction, retrieving the zero-delays prediction beyond the intrinsic resolution of the measurement devices. It should be noted that the effect of not considering the 14.61 ms forward prediction would be sub-millimetric 3D discrepancies, as shown in the Signal time prediction accuracy section. Nonetheless, the comparable duration of each raster point irradiation (10 ms spot duration) would result in visible interplay effects (38) on the deposited dose, which prompted us to consider prediction errors very carefully.

The use of a single marker for the determination of the respiratory phase is a simplified approach allowed by the particular setup, characterized by a remarkable repeatability in the thorax motion (39). This allows for a robust MPh classification considering the proximal surrogate, *i.e.* the one featuring the widest range of motion. However, the implemented framework could be easily extended to the use of more complex strategies based on multiple surface landmarks analysis, as described by Gianoli *et al. (*42).

In our study, the phantom accurate periodical motion ensured optimal setup consistency with the treatment plan over time. In light of future clinical applications, target motion time-invariance assumptions should be verified performing breath-by-breath check of patient respiration period consistency with respect to nominal value. The complementary amplitude-based analysis of motion repeatability implies even further stricter positioning requirements and the definition of clinically reasonable criteria of tolerance margins, which is beyond the scope of the reported study. Deviations from the 'average' motion captured in the treatment planning 4DCT image are critical in particle therapy, where real time plan adaptation is hard to achieve. Particular focus should be addressed to deformations and rotations that will result in dose inhomogeneities despite beam tracking (43). Treatment delivery in presence of breathing irregularities has been tested in Seregni *et al.* (33), relying on the same experimental setup described in this work. Results in presence of baseline drift and phase shift in the target motion show residuals few percent mean dose deviation with respect to static irradiation, when compensated by beam tracking without specific treatment plan adaptation.

The implementation fulfills the technological requirements of up-to-date 4D treatment delivery environment. Target positional information coming from in-room acquisition systems are processed to obtain an accurate time-resolved geometrical feedback. The system is compliant for beam tracking, providing continuous target position as estimated by correlation models, as well as for gated approaches, featuring tools for breathing motion discretization in separate phases (44). Reduced median dosimetric deviation of direct target optical tracking with respect to static irradiation (-0.3%) with narrow IQR 2.3% are reported. These latter represent an experimental verification of the described framework and quantify the bias introduced by the beam tracking approach in motion compensation. Moreover the impact of MPh based discretization of lateral target motion was compared with direct target observation measurements (Figure 7). The decrease in dosimetric homogeneity (IQR: 9.3%) implies further investigation for the clinical feasibility of full motion-phase based compensation, with potentially not negligible dosimetric deviations with respect to in-plane direct target tracking.

Conclusion

A general framework for real time motion tracking in active scanning carbon ion beam therapy has been designed and experimentally validated in a phantom study within the particle therapy workflow for the treatment of moving targets. A custom breathing phantom capable to mimic breathing motion and to simulate an internal moving target was used for the experimental assessment of optically-driven beam tracking with a scanned carbon ion beam. The reported dosimetric results confirm the feasibility of the implemented strategy towards 4D treatment delivery, with expected notable improvement in dose deposition with respect to the non-compensated strategy and few percent residual deviations with respect to static irradiation. The framework has been designed to fulfill the technical specifications of up-to-date motion monitoring system and correlation models.

Conflict of Interests

None.

Acknowledgements

The authors would like to acknowledge the EU-FP7 ULICE project, WP 4: "Ion- therapy for intra-fractionally moving targets" (Grant agreement number 228436) and the German Research Foundation (DFG) (Clinical research unit 214) for partially founding these activities. We further thank the team of the RadioOncology team at the University Hospital in Heidelberg, especially Christopher Kurz, for the 4DCT acquisition of our phantom.

References

1. US National Institutes of Health, National Cancer Institute, DCCPS, Surveillance Research Program, Cancer Statistics Branch. Surveillance, Epidemiology, and End Results (SEER). Program Research Data (1973-2008). http://www.seer.cancer.gov (Accessed: August, 2013).
2. Durante M & Loeffler JS. Charged particles in radiation oncology. *Nat Rev Clin Oncol 7*, 37-43 (2010). DOI: 10.1038/nrclinonc.2009.183
3. Peeters A, Grutters JP, Pijls-Johannesma M, Reimoser S, De Ruysscher D, Severens JL, Joore MA & Lambin P. How costly is particle therapy? Cost analysis of external beam radiotherapy with carbon-ions, protons and photons. *Radiother Oncol 95*, 45-53 (2010). DOI: 10.1016/j.radonc.2009.12.002
4. Pijls-Johannesma M, Grutters JP, Verhaegen F, Lambin P & De Ruysscher D. Do we have enough evidence to implement particle therapy as standard treatment in lung cancer? A systematic literature review. *Oncologist 15*, 93-103 (2010). DOI: 10.1634/theoncologist.2009-0116
5. Loeffler JS & Durante M. Charged particle therapy–optimization, challenges, and future directions. *Nat Rev Clin Oncol 10*, 411-424 (2013). DOI: 10.1038/nrclinonc.2013.79
6. Richter D, Schwarzkopf A, Trautmann J, Kramer M, Durante M, Jakel O & Bert C. Upgrade and benchmarking of a 4D treatment

planning system for scanned ion beam therapy. *Med Phys 40*, 051722 (2013). DOI: 10.1118/1.4800802
7. Bert C, Gemmel A, Saito N, Chaudhri N, Schardt D, Durante M, Kraft G & Rietzel E. Dosimetric precision of an ion beam tracking system. *Radiat Oncol 5*, 61 (2010). DOI: 10.1186/1748-717x-5-61
8. Bert C, Gemmel A, Saito N & Rietzel E. Gated irradiation with scanned particle beams. *Int J Radiat Oncol 73*, 1270-1275 (2009). DOI: 10.1016/j.ijrobp.2008.11.014
9. Grozinger SO, Rietzel E, Li Q, Bert C, Haberer T & Kraft G. Simulations to design an online motion compensation system for scanned particle beams. *Phys Med Biol 51*, 3517-3531 (2006). DOI: 10.1088/0031-9155/51/14/016
10. Bert C & Rietzel E. Compensation of Target Motion. In: Ion Beam Therapy. U. Linz (Ed.), vol. 320, pp. 545-558, Springer, 2012.
11. Riboldi M, Orecchia R & Baroni G. Real-time tumour tracking in particle therapy: technological developments and future perspectives. *Lancet Oncol 13*, e383-391 (2012). DOI: 10.1016/s1470-2045(12)70243-7
12. Rietzel E & Bert C. Respiratory motion management in particle therapy. *Med Phys 37*, 449-460 (2010). DOI: 10.1118/1.3250856
13. Lomax AJ. Intensity modulated proton therapy and its sensitivity to treatment uncertainties 2: the potential effects of inter-fraction and inter-field motions. *Phys Med Biol 53*, 1043-1056 (2008). DOI: 10.1088/0031-9155/53/4/015
14. Zhang Y, Boye D, Tanner C, Lomax AJ & Knopf A. Respiratory liver motion estimation and its effect on scanned proton beam therapy. *Phys Med Biol 57*, 1779-1795 (2012). DOI: 10.1088/0031-9155/57/7/1779
15. Riboldi M, Sharp GC, Baroni G & Chen GT. Four-dimensional targeting error analysis in image-guided radiotherapy. *Phys Med Biol 54*, 5995-6008 (2009). DOI: 10.1088/0031-9155/54/19/022
16. Furukawa T, Inaniwa T, Sato S, Tomitani T, Minohara S, Noda K & Kanai T. Design study of a raster scanning system for moving target irradiation in heavy-ion radiotherapy. *Med Phys 34*, 1085-1097 (2007). DOI: 10.1118/1.2558213
17. Furukawa T, Inaniwa T, Sato S, Shirai T, Mori S, Takeshita E, Mizushima K, Himukai T & Noda K. Moving target irradiation with fast rescanning and gating in particle therapy. *Med Phys 37*, 4874-4879 (2010). DOI: 10.1118/1.3481512
18. Zenklusen SM, Pedroni E & Meer D. A study on repainting strategies for treating moderately moving targets with proton pencil beam scanning at the new Gantry 2 at PSI. *Phys Med Biol 55*, 5103-5121 (2010). DOI: 10.1088/0031-9155/55/17/014
19. Bert C, Grozinger SO & Rietzel E. Quantification of interplay effects of scanned particle beams and moving targets. *Phys Med Biol 53*, 2253-2265 (2008). DOI: 10.1088/0031-9155/53/9/003
20. Grozinger SO, Li Q, Rietzel E, Haberer T & Kraft G. 3D online compensation of target motion with scanned particle beam. *Radiother Oncol 73*(Suppl. 2), S77-79 (2004). DOI: 10.1016/S0167-8140(04)80020-3
21. Li Q, Groezinger SO, Haberer T, Rietzel E & Kraft G. Online compensation for target motion with scanned particle beams: simulation environment. *Phys Med Biol 49*, 3029-3046 (2004). DOI: 10.1088/0031-9155/49/14/001
22. Shirato H, Shimizu S, Kunieda T, Kitamura K, van Herk M, Kagei K, Nishioka T, Hashimoto S, Fujita K, Aoyama H, Tsuchiya K, Kudo K & Miyasaka K. Physical aspects of a real-time tumor-tracking system for gated radiotherapy. *Int J Radiat Oncol 48*, 1187-1195 (2000). DOI: 10.1016/S0360-3016(00)00748-3
23. Shirato H, Oita M, Fujita K, Watanabe Y & Miyasaka K. Feasibility of synchronization of real-time tumor-tracking radiotherapy and intensity-modulated radiotherapy from viewpoint of excessive dose from fluoroscopy. *Int J Radiat Oncol 60*, 335-341 (2004). DOI: 10.1016/j.ijrobp.2004.04.028
24. Balter JM, Wright JN, Newell LJ, Friemel B, Dimmer S, Cheng Y, Wong J, Vertatschitsch E & Mate TP. Accuracy of a wireless localization system for radiotherapy. *Int J Radiat Oncol 61*, 933-937 (2005). DOI: 10.1016/j.ijrobp.2004.11.009
25. Harris EJ, Miller NR, Bamber JC, Symonds-Tayler JR & Evans PM. Speckle tracking in a phantom and feature-based tracking in liver in the presence of respiratory motion using 4D ultrasound. *Phys Med Biol 55*, 3363-3380 (2010). DOI: 10.1088/0031-9155/55/12/007
26. Vedam SS, Keall PJ, Kini VR, Mostafavi H, Shukla HP & Mohan R. Acquiring a four-dimensional computed tomography dataset using an external respiratory signal. *Phys Med Biol 48*, 45-62 (2003). DOI: 10.1088/0031-9155/48/1/304
27. Meeks SL, Tome WA, Willoughby TR, Kupelian PA, Wagner TH, Buatti JM & Bova FJ. Optically guided patient positioning techniques. *Semin Radiat Oncol 15*, 192-201 (2005). DOI: 10.1016/j.semradonc.2005.01.004
28. Rietzel E, Pan T & Chen GT. Four-dimensional computed tomography: image formation and clinical protocol. *Med Phys 32*, 874-889 (2005). DOI: 10.1118/1.1869852
29. Torshabi AE, Pella A, Riboldi M & Baroni G. Targeting accuracy in real-time tumor tracking via external surrogates: a comparative study. *Technol Cancer Res T 9*, 551-562 (2010).
30. Kilby W, Dooley JR, Kuduvalli G, Sayeh S & Maurer CR, Jr. The CyberKnife Robotic Radiosurgery System in 2010. *Technol Cancer Res T 9*, 433-452 (2010).
31. Rosen I & Pino R. Novalis and Varian Systems. In: Stereotactic Body Radiation Therapy. Lo S, Teh B, Lu J & Schefter T (Eds.), pp. 53-65, Springer, 2012.
32. Saito N, Bert C, Chaudhri N, Gemmel A, Schardt D, Durante M & Rietzel E. Speed and accuracy of a beam tracking system for treatment of moving targets with scanned ion beams. *Phys Med Biol 54*, 4849-4862 (2009). DOI: 10.1088/0031-9155/54/16/001
33. Seregni M, Kaderka R, Fattori G, Riboldi M, Pella A, Constantinescu A, Saito N, Durante M, Cerveri P, Bert C & Baroni G. Tumor tracking based on correlation models in scanned ion beam therapy: an experimental study. *Phys Med Biol 58*, 4659-4678 (2013). DOI: 10.1088/0031-9155/58/13/4659
34. Fattori G, Riboldi M, Desplanques M, Tagaste B, Pella A, Orecchia R & Baroni G. Automated fiducial localization in CT images based on surface processing and geometrical prior knowledge for radiotherapy applications. *IEEE T Bio-Med Eng 59*, 2191-2199 (2012). DOI: 10.1109/tbme.2012.2198822
35. Fitzpatrick JM, West JB & Maurer CR, Jr. Predicting error in rigid-body point-based registration. *IEEE T Med Imaging 17*, 694-702 (1998). DOI: 10.1109/42.736021
36. Bert C, Saito N, Schmidt A, Chaudhri N, Schardt D & Rietzel E. Target motion tracking with a scanned particle beam. *Med Phys 34*, 4768-4771 (2007). DOI: 10.1118/1.2815934
37. Bert C & Rietzel E. 4D treatment planning for scanned ion beams. *Radiother Oncol 2*, 24 (2007). DOI: 10.1186/1748-717x-2-24
38. Saito N, Chaudhri N, Gemmel A, Durante M, Rietzel E & Bert C. Prediction methods for synchronization of scanned ion beam tracking. *Phys Medica* (2012). DOI: 10.1016/j.ejmp.2012.08.003
39. Steidl P, Richter D, Schuy C, Schubert E, Haberer T, Durante M & Bert C. A breathing thorax phantom with independently programmable 6D tumour motion for dosimetric measurements in radiation therapy. *Phys Med Biol 57*, 2235-2250 (2012). DOI: 10.1088/0031-9155/57/8/2235
40. Riboldi M, Baroni G, Spadea MF, Bassanini F, Tagaste B, Garibaldi C, Orecchia R & Pedotti A. Robust frameless stereotactic localization in extra-cranial radiotherapy. *Med Phys 33*, 1141-1152 (2006). DOI: 10.1118/1.2181299
41. Bert C, Richter D, Durante M & Rietzel E. Scanned carbon beam irradiation of moving films: comparison of measured and calculated response. *Radiother Oncol 7*, 55 (2012). DOI: 10.1186/1748-717x-7-55

42. Gianoli C, Riboldi M, Spadea MF, Travaini LL, Ferrari M, Mei R, Orecchia R & Baroni G. A multiple points method for 4D CT image sorting. *Med Phys 38*, 656-667 (2011). DOI: 10.1118/1.3538921
43. Lüchtenborg R, Saito N, Durante M & Bert C. Experimental verification of a real-time compensation functionality for dose changes due to target motion in scanned particle therapy. *Med Phys 38*, 5448-5458 (2011). DOI: 10.1118/1.3633891
44. Graeff C, Durante M & Bert C. Motion mitigation in intensity modulated particle therapy by internal target volumes covering range changes. *Med Phys 39*, 6004-6013 (2012). DOI: 10.1118/1.4749964

Received: September 2, 2013; Revised: October 9, 2013; Accepted: October 10, 2013